

Effects of sonication energy on the dispersion of carbon nanotubes in a vinyl ester matrix and associated thermo-mechanical properties

S. M. Sabet¹ · H. Mahfuz¹ · J. Hashemi¹ · M. Nezakat² · J. A. Szpunar²

Received: 23 December 2014 / Accepted: 13 April 2015 / Published online: 21 April 2015
© Springer Science+Business Media New York 2015

Abstract In the present paper, we report a systematic examination of sonication energy and the subsequent dispersion condition of nanoparticles in a vinyl ester resin. The nanoparticles were multi-walled carbon nanotubes (MWCNTs) functionalized with carboxylic acid groups. Two nanoparticle concentrations of 0.25 and 0.5 wt% with a variety of sonication amplitudes and duration were considered. Elastic moduli were determined using a 3-point flexural method and a nanoindentation technique. Glass transition temperatures (T_g) were also evaluated by differential scanning calorimetry. The dispersion quality of MWCNTs was investigated by high-resolution scanning electron microscopy (HR-SEM). Results indicated that with both concentrations, there is a gradual increase in elastic modulus and T_g up to a certain sonication energy level beyond which both properties decreased. However, this threshold energy level varied with MWCNT concentration. For example, the threshold energy level was 60 kJ in case of 0.25 wt% while it was only 15 kJ with 0.5 wt% concentration. It was also observed that regardless of the level of threshold energy, enhancement in properties remained more or less the same. This suggests that there is interplay between particle concentration and sonication energy that dictates the dispersion condition and hence controls the nanocomposite properties. It is further

evidenced by SEM studies that nanotubes undergo significant structural changes such as length reduction even at lower energies that eventually limits the threshold level.

Introduction

Since the discovery of carbon nanotubes (CNTs), numerous studies have been conducted to obtain CNT-polymer nanocomposites with outstanding multi-functional characteristics [1, 2]. Due to fibrous shape, excellent mechanical properties, and large specific surface area of nanotubes, CNT-enhanced polymer nanocomposites can be expected to show considerably improved mechanical properties compared with the neat matrix material [3, 4]. To realize the promising potentials of CNTs, it is important to achieve highly exfoliated CNT bundles as well as homogeneous distribution of nanotubes followed by their integration into the molecular structure of polymeric matrix [5–9]. Particularly, the dispersion of CNTs helps determine the optimal reinforcing effect. Carbon nanotubes tend to aggregate in a matrix due to their small size and the strong van der Waals (vdW) interaction between nanotubes [10–12]. Thus, a uniform dispersion of CNTs is still one of the challenges in research associated with CNT-reinforced composites that must be resolved.

Ultrasonication is a common technique to break up the CNT bundles in low-viscosity resins using the acoustic cavitation mechanism. The cavitation involves the formation, expansion, and implosion of numerous microscopic bubbles, which result in the generation of attenuated waves [13]. Although the amount of energy released by each individual bubble is minimal, the cumulative energy can be high enough to induce powerful shock waves in the molecules of the resin. The production of these shock

✉ H. Mahfuz
hmahfuz@fau.edu

¹ Department of Ocean and Mechanical Engineering, Florida Atlantic University, 777 Glades Road, Boca Raton, FL 33431, USA

² Department of Mechanical Engineering, University of Saskatchewan, 57 Campus Dr, Saskatoon, SK S7N 1L5, Canada

waves promotes the peeling off individual CNTs located at the outer part of the nanotube bundles or agglomerates, and thus results in the separation of individualized nanotubes from the bundles. Cavitation intensity and the efficiency of the sonication process depend on the equipment used as well as the physical properties of the resin [14, 15].

Large-scale engineering composite structures often use vinyl ester (VE) as a primary resin system because of its low cost and low viscosity, making it suitable for most synthesizing processes [16]. To date, few researches have focused on CNT dispersion in VE matrix through different fabrication processes. Seyhan et al. [17, 18] successfully employed a 3-roll milling technique to disperse CNTs into a VE/polyester hybrid resin. Fan et al. [19, 20] examined the influence of different processing techniques on the dispersion of CNTs in VE resin. They reported that acid oxidized nanotubes can be dispersed homogeneously in the matrix because nanotube length is reduced during the acid reflux. Gryshchuk et al. [21] investigated VE nanocomposites with mechanical stirring and ultrasonic mixing. Poor nanotube dispersion was reported in the VE system due to nano-scale entanglement. Minor increases in the elastic properties and the fracture toughness at varying nanotube concentrations were reported. A number of studies also reported an improved dispersion state of CNTs by the surface treatment of nanotubes prior to the sonication process [22–24].

Although the ultrasonication process has been used in the past to disperse CNTs in the VE matrix, this process has not been optimized. According to the best knowledge of authors, there has not been a thorough investigation of the effect of sonication conditions, i.e., duration and amplitude on the CNT dispersion. Therefore, the purpose of the present study is to systematically investigate this effect. In this regard, ultrasonication mixing method is employed to synthesize CNT/VE nanocomposites containing two CNT concentrations, namely 0.25 and 0.5 wt%. A variety of sonication parameters are selected to produce different nanotube dispersion states. The mechanical and thermal properties and the fracture behavior of the experimental materials are evaluated. For deeper understanding of the observed results, the nanotube dispersion quality is examined through scanning electron microscopy (SEM).

Materials and methods

Materials

Multi-walled carbon nanotubes (MWCNTs) with >8 at.% carboxylic acid functional groups were provided by Sigma-Aldrich. The as-received MWCNTs have a mean diameter of ~9.5 nm and length of ~1.5 μm. The thermosetting

matrix used was a Derakane 8084 epoxy vinyl ester resin from Ashland Composites (Dublin, Ohio, USA) containing ~40 wt% styrene. In accordance with the supplier data-sheet, methyl ethyl ketone peroxide (MEKP), Cobalt Naphthenate—6 % (CoNap—6 %), and dimethylaniline (DMA) were used as curing agents.

Preparation of CNT/VE nanocomposites

Nanocomposite specimens with different CNT contents namely 0, 0.25, and 0.5 wt% were fabricated as follows. Measured amount of CNT powder was dispersed in the VE resin first by mechanical stirring and then by ultrasonication. The total mass of the mixture was 15 g. The sonication was carried out in a Sonics Vibra Cell liquid processor (Ti-horn, frequency of 20 kHz). In order to avoid a rise in the temperature during sonication, the mixing beaker was kept inside a 6 °C water bath. A variety of mixing times and amplitudes were examined to determine the optimal sonication parameters. The sonication times, amplitudes, and the corresponding total sonication energy are shown in Table 1.

The sonication processor continuously displays the actual amount of power that is being delivered to the probe. During sonication at 50 and 70 % amplitude, an output power of 35–38 and 55–57 W, respectively, was recorded. The total sonication energy was calculated by multiplying the output power by mixing time, according to Eq. 1:

$$\text{Total energy (J)} = \text{power (W)} \times \text{mixing time (s)} \quad (1)$$

For example, during sonication of a 0.25 wt% CNT–VE mixture at 50 % amplitude for 18 min, an average power of 37 W was recorded. Therefore, the total energy input would be $E_{\text{tot}} = 37 \text{ (W)} \times 18 \times 60 \text{ (s)} = 39,960 \text{ J} \approx 40 \text{ kJ}$.

After sonication, CNT/VE mixtures were degassed under vacuum for approximately 20 min, and then mixed with curing agents before casting into the mold. Subsequently, the mixtures were cured for 24 h at room temperature and post-cured for 2 h at 99 °C.

Testing

Room temperature mechanical properties of the neat VE polymer and its composites were measured according to ASTM D790-10 [25]. A Zwick/Roell universal tension–compression testing machine with 3-point flexural setup was employed. Testing was performed with a support span-to-depth ratio of 16:1 and crosshead speed of 0.5 mm min⁻¹.

Nanoindentation tests were also performed following ASTM E2546-07 [26] using a NANOVEA hardness tester (Nanovea, CA, USA), equipped with a Berkovich indenter

Table 1 Different sonication parameters examined in this study

MWCNT (wt%)	Sample	Sonication parameter		
		Duration (min)	Amplitude (%)	Energy (kJ)
0	Neat VE	–	–	0
	0.25–10	3	70	10
	0.25–20	9	50	20
0.25	0.25–40	18	50	40
	0.25–60	18	70	60
	0.25–80	24	70	80
	0.5–10	4	50	10
	0.5	0.5–15	7	50
0.5	0.5–20	7	70	20

tip. Samples for indentation tests were cut and mounted on a holder. In order to obtain a good surface finish, samples were successively polished using 6, 3, 1, and 0.25 μm diamond paste. All nanoindentation tests were performed with a maximum normal load of 800 μN and a constant loading/unloading rate of 25 μN s⁻¹. The elastic modulus (*E*) can be calculated from the following equations [26]:

$$\frac{1}{E_r} = \frac{1 - \nu^2}{E} + \frac{1 - \nu_i^2}{E_i} \tag{2}$$

$$E_r = \frac{\sqrt{\pi} dP}{2 dh \sqrt{A}}, \tag{3}$$

where *E_r* is the reduced modulus of indentation contact, *E_i* (1140 GPa) and *ν_i* (0.07) are the elastic modulus and Poisson’s ratio of the diamond indenter, *ν* = 0.35 [27] is the Poisson’s ratio of the VE polymer, *S* = *dP/dh* is the contact stiffness, and *A* is the projected contact area at the maximum load. Prior to experiments, the tip area function was calibrated using Oliver and Pharr method [28]. In order to reduce the creep effect, the maximum load was kept constant for 10 s. A quite number of indentations were made on each type of sample on random locations to obtain reliable results.

The fracture surfaces of flexural specimens were examined using high-resolution scanning electron microscopy (Hitachi SU6600 Analytical VP FEG-SEM) to study the surface roughness, the CNT dispersion state, and active fracture mechanisms. The fracture surfaces were sputter-coated with gold prior to observation.

A TA Instrument Q-10 differential scanning calorimetry apparatus was used to determine the glass transition temperature (*T_g*) of the experimental materials. Three samples (10–15 mg each) were prepared from each post-cured block and tested for the measurements using an aluminum empty pan as a reference. Each sample was heated from 0 up to 200 °C with a constant heating rate of 10 °C min⁻¹. After cooling down to room temperature, a similar heating cycle was applied on the sample and the data were recorded. The *T_g* values were determined according to ASTM D7426-08 [29].

Results and discussion

Flexural behavior

Typical flexural stress–strain curves of the pure polymer and its nanocomposites are illustrated in Fig. 1. As expected from the brittle nature of thermosetting polymers [30], both the neat VE and its nano-modified systems behave in a typical brittle manner with limited plastic deformation. According to the graphs, the incorporation of CNTs reduces the ductility of the pure polymer. This is more pronounced in the system with 0.5 wt% CNT reinforcement. By adding the stiff nanotubes into the polymer matrix, the regions of high CNT concentration act as local stress concentration sites, and thus promote crack initiation [18]. Consequently, the material fails before reaching the ultimate flexural strength. However, a detailed microstructural investigation of the fractured specimens has been performed to identify the involved mechanisms.

Figure 2 shows the representative SEM micrographs of the fracture surface of the VE polymer and a nanocomposite fabricated with 0.5 wt% CNTs. In Fig. 2a, the presence of river marks on a relatively smooth fracture surface of the pure VE specimen indicates a predominantly brittle fracture mode. The river patterns are highlighted in the figure by arrows. The fracture surface of the nanocomposite (Fig. 2b), however, shows substantial increase in the surface roughness, implying that the crack propagation was opposed or resisted by CNT reinforcement [31]. The red arrow in Fig. 2b shows the initial crack nucleation site as well as the crack propagation direction. The nucleation of the initial crack seems to have started from a CNT agglomeration at the tension side of the specimen. A narrow region (Zone I) of torn surfaces with nonlinear deformation paths surrounding the initial crack can be recognized. As the crack propagates, a new region appears on the fracture surface, Zone II, which is covered by the outwardly expanding microcracks with dimpled patterns. Detailed SEM analysis demonstrates that at this stage of

Fig. 1 The effect of sonication conditions on the flexural behavior of composites containing **a** 0.25 wt% and **b** 0.5 wt% CNTs

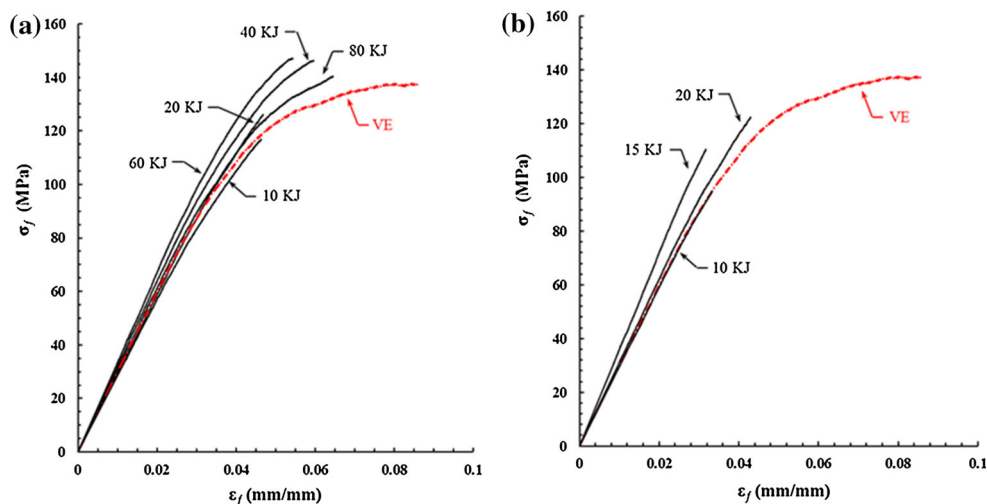
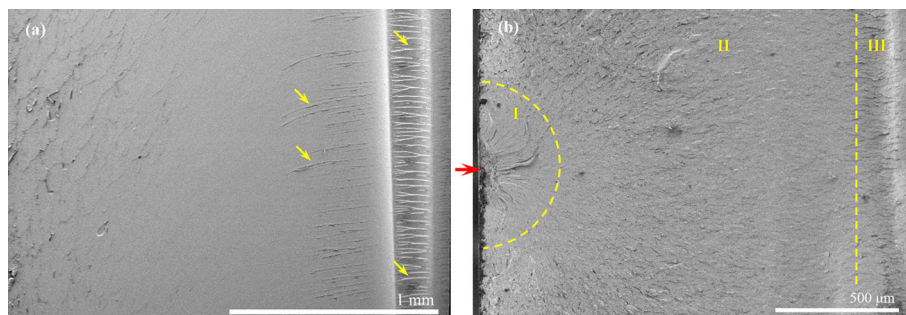


Fig. 2 SEM micrographs of the fracture surface of **a** the neat VE polymer and **b** nanocomposite fabricated with 0.5 wt% CNT content (Color figure online)



the fracture, the highly textured surface is possibly generated by sequential nucleation, growth, and coalescence of microcracks. A remarkable amount of fracture energy can be dissipated through the generation of additional fracture surfaces [32]. Finally, a relatively smooth surface with river patterns can be recognized at the compression side of the specimen, Zone III.

To better understand the effect of sonication parameters, the following approach was considered. Based on the linear part of the flexural stress–strain curves, the flexural moduli of the neat VE and CNT-modified nanocomposites were calculated. In addition, the average elastic modulus of each material was determined using nanoindentation testing method. The idea of two parallel studies using flexural and nanoindentation techniques is to estimate the effect of CNT reinforcement in the matrix in a bulk as well as in a local context. In flexural tests, a large volume of the material is subjected to linearly varying stress field and the measured properties are indeed bulk properties, whereas in nanoindentation tests, the modulus measurement is from the response of a small volume of the material as encountered by the indenter tip as discussed in “Testing” section—making it very much local. It is believed that these two aspects, i.e., bulk and local, can best cover the dispersion issues. At each

CNT content, the variations of the flexural strength and the modulus with sonication parameters were studied. Moreover, the microstructural evolution and the fracture behavior of the composite materials were carefully investigated by SEM analysis.

The 0.25 wt% CNT/VE nanocomposites

The effect of sonication parameters on the elastic modulus of nanocomposites with 0.25 wt% CNT is summarized in Fig. 3. For comparison, the measured modulus of the pure polymer is also presented. The neat VE polymer possesses an average flexural and indentation modulus of 2.99 and 3.5 GPa, respectively. It is clear from the results that the measured moduli from indentation tests are higher than those obtained from flexural tests. In nanoindentation tests, a highly non-uniform stress field is generated around the indenter tip due to the complex shape of the Berkovich indenter. Moreover, the nanoindentation modulus is measured from the slope of unloading curve in the load–penetration graph [26]. In contrast, in 3-point bending, a linearly varying stress field is encountered during the test and the flexural modulus is measured using global deflection of the sample. Therefore, the moduli measured from

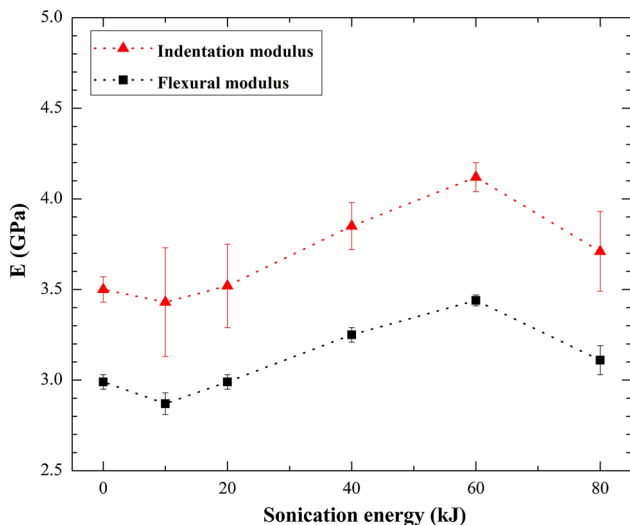


Fig. 3 The effect of sonication energy on the elastic modulus of composites synthesized with 0.25 wt% CNT content (The values at zero sonication energy are associated with the neat VE moduli)

two different methods will be different. Higher modulus measured from nanoindentation is attributed to complex material plasticity during penetration of the indenter, as indicated in the literature [33–35].

As mentioned before, a very small volume of the material is deformed during penetration of the indenter. The elastic modulus is measured from the deformation behavior of this microscopic volume. Since the chances of hitting nanotubes in this volume would be different at different locations, inherently the data will give a relatively large error bar. On the contrary, 3-point bending tests determine the modulus and strength where a large volume of the specimen is taken into consideration. As a consequence, the error bar is smaller. It is also evident that the indentation modulus variation with sonication energy presents a similar trend to that observed for the flexural modulus.

A slight drop in the modulus is found at an energy level of around 10 kJ, corresponding to the sonication for 3 min at 70 % amplitude. Figure 4 presents the fracture surface of this specimen. A poor CNT dispersion condition with separate CNT agglomerates (red arrows in Fig. 4a) can be detected in the surrounding matrix resin. Because of the high specific surface area (SSA) of the nanotubes as well as their high polarizability [2], the amount of energy required to separate an individual tube from the agglomerate is considerable. Thus, in the absence of strong favorable interactions between the tubes and the polymer matrix, the preferred configuration of tubes in a polymer will be in a bundled arrangement at sufficient nanotube concentration [12]. Moreover, in-depth SEM analysis reveals that the agglomerates of CNTs exhibit a relatively weak adhesion to the matrix, so that an extensive de-bonding and matrix cracking (indicated in Fig. 4b by arrows) occur around the

agglomerates. The slight drop in the modulus can be attributed to the poor dispersion of nanotubes and their weak adhesion to the VE matrix. The early failure of the specimen due to the aforementioned mechanisms can also be responsible for a remarkable drop in the flexural strength of the material (Fig. 1a, 10 kJ).

The results show that sonication at 20 kJ does not influence the elastic modulus and flexural strength of the composite, comparing to those of the neat VE resin. By doubling the mixing time from 9 to 18 min at constant amplitude of 50 %, and thus doubling the sonication energy to 40 kJ, the mechanical properties show an ascending trend. An improvement of about 6 and 9 % is achieved in the flexural strength and modulus, respectively. Figure 5 presents the fracture surface of specimens fabricated at the constant amplitude of 50 % and sonicated at various durations. According to Fig. 5a, some individual CNTs are visible around a partially disentangled agglomerate. By comparing this micrograph with the microstructure of Fig. 4, it is evident that the dispersion of nanotubes is slightly enhanced after sonication at 50 % for 9 min. Although the application of higher sonication energy leads to a better CNT dispersion state, the de-bonding of the agglomerate from the surrounding matrix is still detectable (Fig. 5a). It can be conceived that more than one mechanism with opposite effects have been activated during the deformation, resulting in the mechanical properties of the specimen to be close to those of the pure resin, see Figs. 1a and 3 (20 kJ).

As illustrated in Fig. 5b and Table 1, sonication for longer time up to 18 min provides the required energy to break up the nanotube entanglements and improves the CNT dispersion state. The isolated CNTs are in both forms of broken segments (bright dots indicated by red arrows) and curled ropes (indicated by yellow arrows). The presence of small agglomerates is still obvious. Improvement of nanotube dispersion is believed to increase the required load to the failure of the specimen, resulting in an enhancement of the flexural strength (Fig. 1a, 40 kJ). Furthermore, the high degree of CNT disentanglement provides an extensive interfacial area between the CNTs and the polymer matrix. In this condition, the well-dispersed, stiff nanotubes can reduce the mobility of the surrounding polymer chains to some extent [17], leading to an increase in the elastic modulus of the material. These results are in agreement with those previously published on the effect of sonication time on the mechanical properties of different MWCNT-modified polymer systems [36, 37].

Further increase in the modulus (~15 %, comparing to the pure resin) can also be achieved at 60 kJ, i.e., by sonication at 70 % amplitude for the same duration of 18 min. However, longer sonication at 70 % amplitude is found to have a detrimental effect on the mechanical

Fig. 4 SEM micrograph of the fracture surface of composite with 0.25 wt% CNT content sonicated at 70 % amplitude for 3 min (10 kJ) (Color figure online)

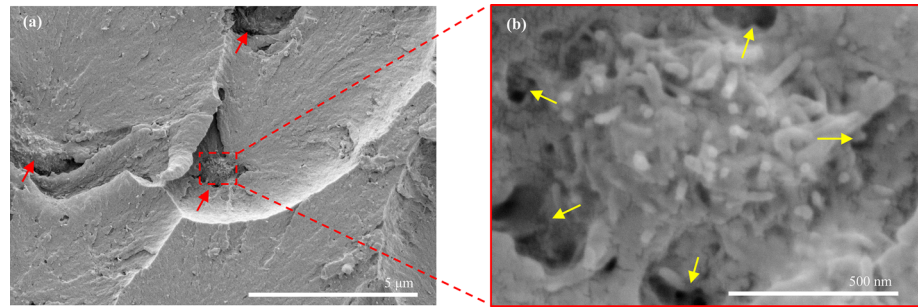
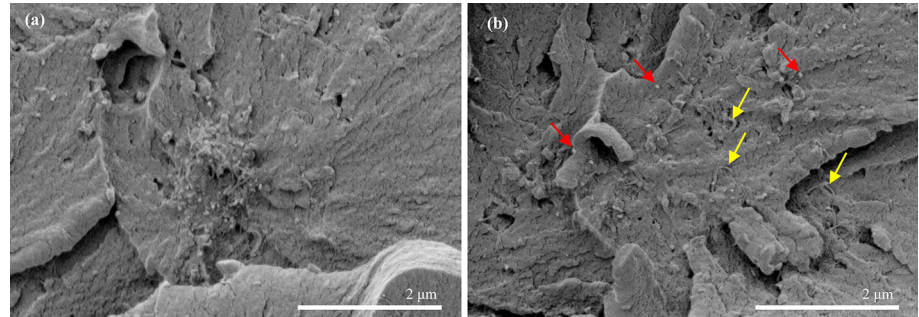


Fig. 5 SEM micrographs of the fracture surface of composites with 0.25 wt% CNT content sonicated at 50 % amplitude for **a** 9 min (20 kJ) and **b** 18 min (40 kJ) (Color figure online)

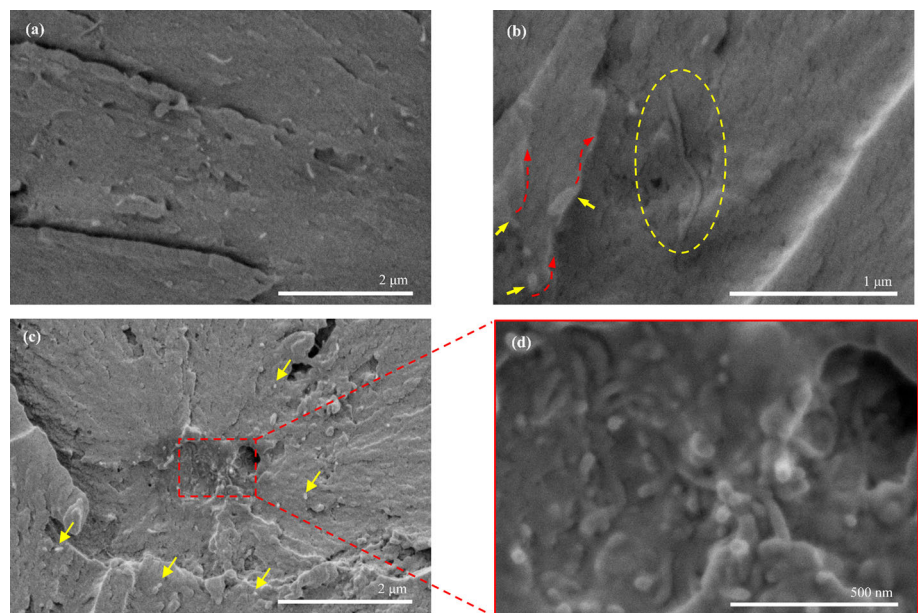


properties. To identify the reasons of the observed behaviors, SEM micrographs of the fracture surface of these specimens are presented in Fig. 6.

A completely disentangled agglomerate is detected in Fig. 6a. The in-depth SEM analysis reveals the presence of isolated, well-dispersed nanotubes on the fracture surface of this specimen. The majority of the nanotubes exhibit short protruding lengths out of the matrix, implying their rupture either during prolonged sonication or during the

fracture. Principally, fillers with stronger interfacial adhesion tend to be fractured under loading [38]. In fact, the carboxylic acid functional groups attached to the outer wall of MWCNTs can facilitate the formation of a relatively strong interfacial adhesion of the nanotube to the surrounding matrix [23]. Consequently, these CNTs are fractured during the crack propagation. Besides, a few nanotubes possess relatively long protruding lengths, indicating that they were failed by a pull-out mechanism.

Fig. 6 SEM micrographs of the fracture surface of composites with 0.25 wt% CNT content sonicated at 70 % amplitude for **a, b** 18 min (60 kJ) and **c, d** 24 min (80 kJ) (Color figure online)



This mechanism usually occurs in the absence of a good interfacial adhesion [31]. Once the CNT bridges the crack tip, one side of the nanotube is completely pulled out from the polymer matrix. As a result, a protruded nanotube and a hole appear on the fracture surface, indicated by oval in Fig. 6b.

Another interesting observation in this micrograph is the occurrence of bifurcation mechanism. During the crack propagation, individual nanofillers can resist the propagation by this mechanism [39–41]. As demonstrated in Fig. 6b, a typical crack tip bifurcation (indicated by dotted red arrows) starts with isolated, well-dispersed nanotubes (indicated by yellow arrows). It is believed that the energy dissipation due to the crack bifurcation enhances the elastic modulus of the composite material [31]. Based on the explanation above, it is suggested that a remarkable dispersion improvement in addition to an extensive crack bifurcation by individual CNTs can be responsible for the observed increase in the mechanical properties of the composite in this condition.

Further sonication up to 24 min at constant amplitude of 70 % (80 kJ, Fig. 6c, d) may have some adverse effects on the CNT dispersion state and their morphology. Generally, two effects can be identified from the SEM micrographs. Although the CNT dispersion is overall satisfactory, it seems that a re-agglomeration process occurred. Some local regions containing high density of entangled CNTs (Fig. 6d) appear within the isolated, broken nanotubes (indicated by arrows in Fig. 6c). The re-agglomeration of CNTs in thermosetting polymers has been previously reported [13, 42, 43]. Li et al. [42] have observed the re-agglomeration process in a CNT/epoxy system after a sequential synthesizing method including CNT surface treatment, sonication, and shear mixing. They have suggested that the disentangled CNTs without sufficient surface functional groups tend to re-agglomerate due to vdW and Coulomb attractions. The existence of some nanotubes without sufficient carboxylic acid functional groups was revealed earlier (Figs. 5b, 6b). These nanotubes are believed to be capable for re-bundling at over-sonication condition (with the total energy of 80 kJ), which can deteriorate the mechanical properties of the composite.

Moreover, a CNT length reduction is apparent in the micrographs of the specimen sonicated for long duration at high amplitude of 70 %. It is generally accepted that the high energy of sonication often results in CNT damage and degrades the structure of the nanotubes [12, 14, 44], which in turn could eventually reduce their length, and therefore deteriorate both the electrical and mechanical properties of the material. In this regard, Battisti et al. [45] have reported an increase in the electrical resistivity of a MWCNT/polyester system with 0.25 wt% nanotube under over-sonication condition. They proposed that at the latest stage

of the sonication process, the eventual damage to the CNT structure could be responsible for the observed behavior. Based on the explanations above, one can conclude that the localized re-agglomeration of CNTs as well as the remarkable reduction of their length may play a significant role in decreasing the mechanical properties of the composite material under excessive sonication (Figs. 1a, 3, 80 kJ).

The 0.5 wt% CNT/VE nanocomposites

Figure 7 illustrates the variation of the elastic modulus with sonication energy for the composites fabricated with 0.5 wt% CNTs. The corresponding SEM images of the fracture surface of these specimens under flexural testing are presented in Fig. 8.

After sonication at a low energy level of 10 kJ (4 min at 50 % amplitude), the modulus remains unaffected being close to that of the neat resin, whereas there was a slight drop in the modulus of 0.25 wt% CNT composite under the same sonication condition. Figure 8a shows a partially disentangled agglomerate. Similar to the 0.25 wt% CNT system, the de-bonding between the agglomerate and the matrix is detectable. It is believed that the drop in the modulus is due to poor CNTs dispersion as well as their weak adhesion to the matrix. Weak dispersion would lead to agglomeration of CNTs, which might behave more like defects. Besides, adhesion to the matrix plays a significant role in controlling the modulus. By comparing the fracture surfaces of 0.25 and 0.5 wt% CNT samples at 10 kJ (Figs. 4, 8a), it can be realized that the de-bonding between agglomerates and the VE matrix is less pronounced in the

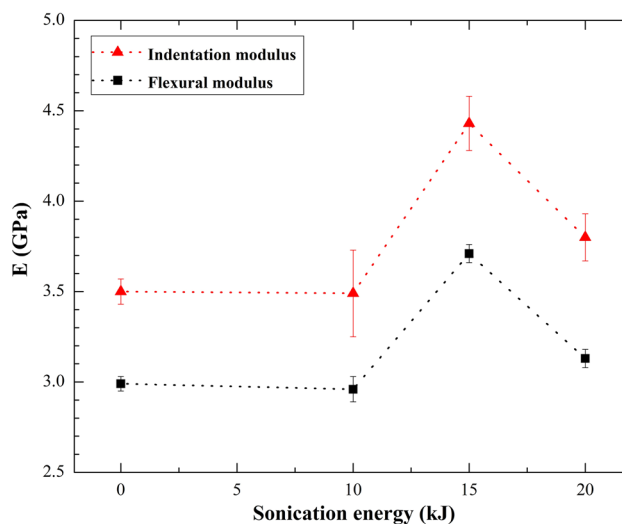
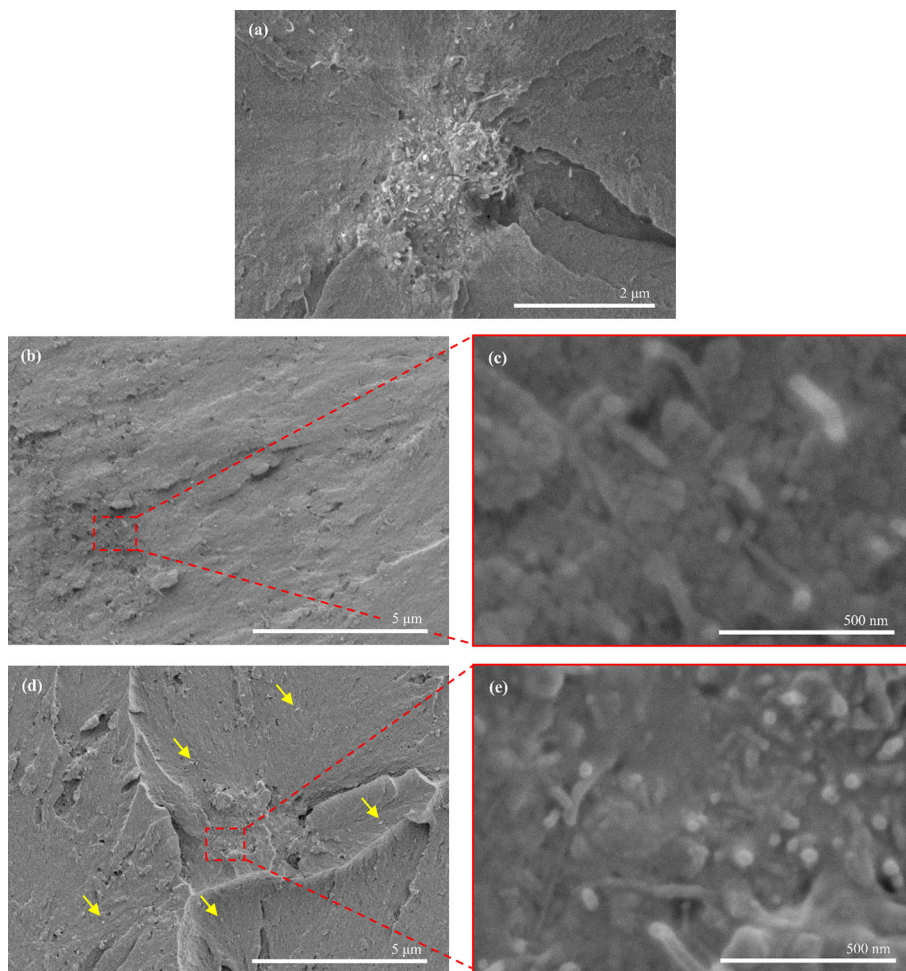


Fig. 7 The effect of sonication parameters on the elastic modulus of composites synthesized with 0.5 wt% CNT content (The values at zero sonication energy are associated with the neat VE moduli)

Fig. 8 SEM micrographs of the fracture surface of composites with 0.5 wt% CNT content sonicated at 50 % amplitude for **a** 4 min (10 kJ), **b**, **c** 7 min (15 kJ), and **d**, **e** at 70 % amplitude for 7 min (20 kJ) (Color figure online)



0.5 wt% CNT composite. Less de-bonding means CNT bundles will still carry some load to maintain the modulus at 0.5 wt% concentration.

However, further mixing up to 7 min at constant amplitude of 50 % (15 kJ) can significantly enhance the modulus, which is as high as ~ 24.1 % more than the pure resin. The corresponding microstructure of the fractured specimen exhibits the breakup of the nanotube agglomerates, Fig. 8b. It can be demonstrated from Fig. 8c that CNTs are agglomerated with the VE resin to bundle (30–50 nm diameter), which is much larger than the as-received MWCNTs (~ 9.5 nm). This suggests that the nanotubes were held tightly to the matrix, demonstrating a strong interaction between the VE matrix and the functionalized nanotubes. Inducing higher sonication energy up to 20 kJ seems to have a distinct effect on destroying the CNTs. The fracture surface at this condition reveals a high number of broken, individually dispersed CNTs (bright dots specified by arrows in Fig. 8d) as well as a region of entangled nanotubes (Fig. 8e). However, the CNT entanglement regions are smaller than those shown in Fig. 8a, and thus, the flexural strength and modulus are improved due to a better dispersion state.

The dispersed CNTs as seen in SEM image of the fracture surfaces can be either non-functionalized or functionalized. It is generally accepted that the functionalized CNTs can make a stronger bonding to the matrix, compared to non-functionalized ones. Therefore, the functionalized CNTs can be detected in SEM images with two main features; (a) broken segments rather than pulled-out ropes, and (b) coated by surrounding matrix and appearing like ropes with larger diameter. The percentage of functionalized CNTs may be statistically estimated by visual inspection of several SEM images from well-dispersed regions, and counting the CNTs with the two distinct features mentioned above. In this study, the average ratio of the functionalized CNTs to all nanotubes detected in SEM images has been estimated to be 77 %.

Nanoindentation curves

To further study the mechanical behavior, nanoindentation results of samples 0.25–60 and 0.5–15 are compared with the neat VE polymer in Fig. 9. According to Fig. 9a, at higher CNT content, the load–displacement curve is shifted to the left and the slope of unloading curve is increased. It

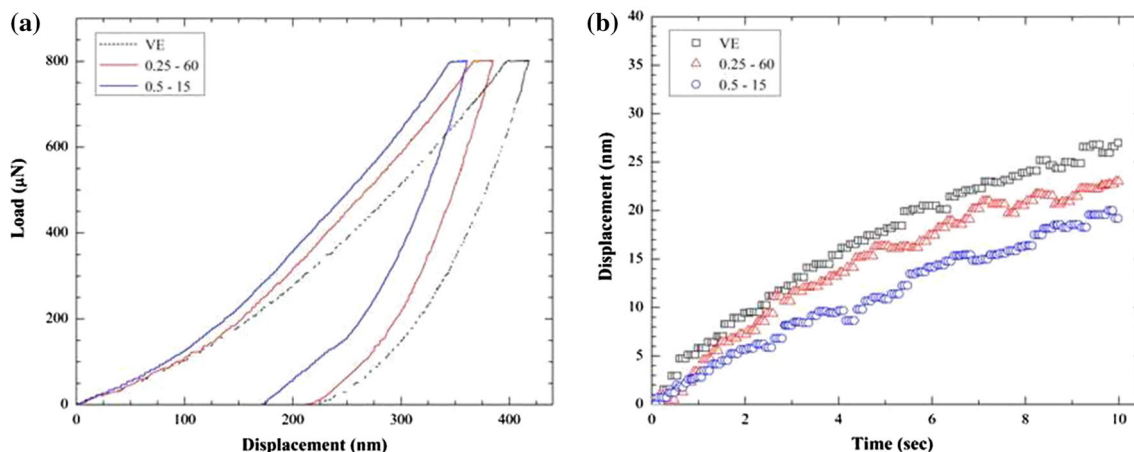


Fig. 9 **a** Representative load–displacement curves derived from nanoindentation tests, and **b** nanoindentation creep deformation at maximum load of 800 μN

is well known that the elastic modulus and the slope of unloading curve (i.e., stiffness) have a direct relationship [26]. Therefore, a growth in stiffness will result in a higher modulus. Microstructural investigations have revealed that these nanocomposite samples possess the most efficient dispersion condition among those with the same CNT content (see Figs. 6a, 8b). As expected, a higher amount of CNTs with an efficient dispersion in the resin matrix can effectively increase the required load for the indenter tip to penetrate into the surface. Thus, the elastic modulus will increase.

The displacement–time data under constant indentation creep load is illustrated in Fig. 9b. Addition of CNTs results in a significant decrease in creep deformation of the pure polymer. This is more pronounced at 0.5 wt% nanotube content, where ~32 % reduction of creep deformation is achieved. The ability of the CNT additives to increase the creep resistance of an epoxy resin has also been reported [46]. This effect may be attributed to several factors. The confinement effect of the highly elastic CNTs can prevent the deformation of the VE network. In other words, CNTs act as the blocking sites that restrict the viscous flow of the VE when subjected to an external indentation force. Moreover, the large interfacial area as a result of effective dispersion can contribute to a significant interface adhesion between individual MWCNTs and the matrix. The latter can improve the load transfer mechanism [47], and thus results in a remarkable enhancement in the creep resistance.

Thermal properties

Figure 10 shows the result of DSC experiments on the pure VE polymer and its nano-modified systems. The post-cured

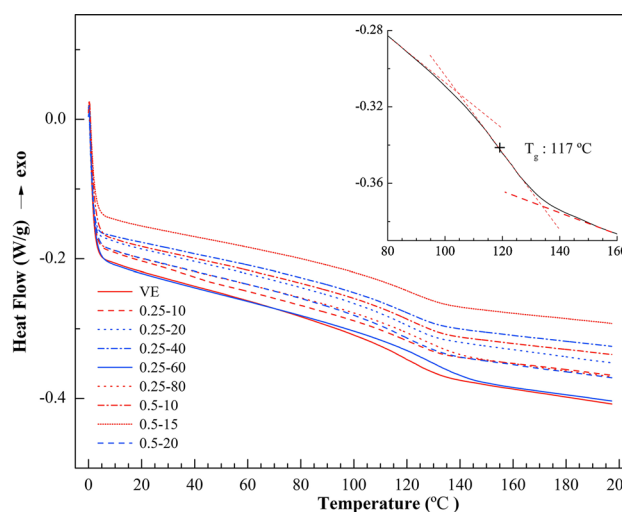


Fig. 10 The DSC heating curves of the neat VE polymer and its composites (at heating rate of 10 °C min⁻¹)

pure polymer exhibits a T_g of ~117 °C (inset, Fig. 10), which is close to the reported value by the manufacturer (115 °C). The variation in the T_g as a function of total sonication energy for the experimental nanocomposites is shown in Fig. 11. As is observed, two distinct zones are identified at each CNT content. The T_g is elevated first with introducing more sonication energy. After reaching a peak value, the T_g falls. The maximum improvement in the T_g (~13 °C) belongs to the composite fabricated with 0.25 wt% CNT with a total energy of 60 kJ, corresponding to sonication at 70 % for 18 min.

The observed behavior can be correlated to the CNT dispersion quality. It can be generally noticed that an increase in the disentanglement of CNT agglomerates will result in a higher T_g . For instance, nanocomposite samples 0.25–60 and 0.5–15 were known to have the most efficient

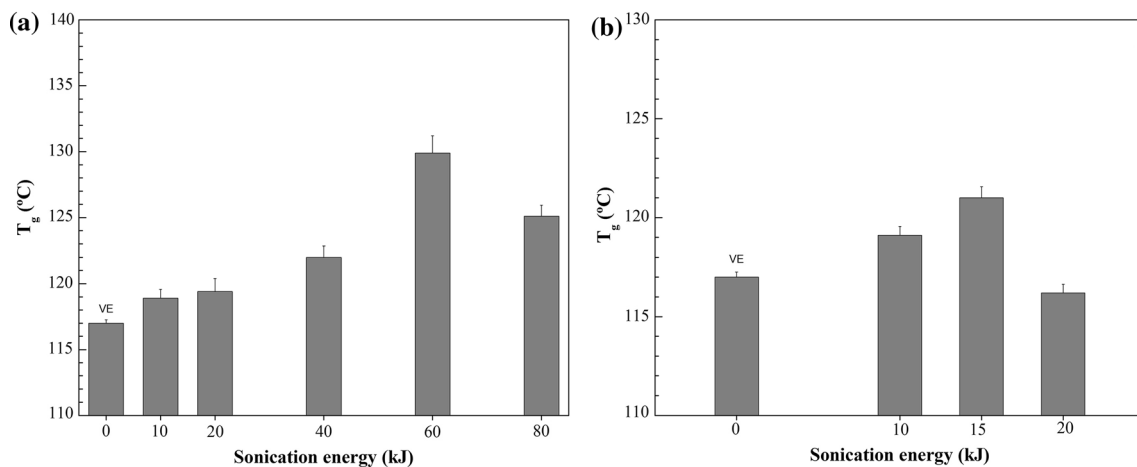


Fig. 11 The T_g of the composites with **a** 0.25 wt% and **b** 0.5 wt% CNT content as a function of total sonication energy

CNT dispersion, and hence, they hold the highest T_g values at 0.25 and 0.5 wt% CNT systems, respectively. As mentioned earlier, an effective dispersion of the CNTs can provide a large interfacial area between individual nanotubes and their surrounding matrix. In this condition, the nanotubes form an infiltrating network of cross-linking elements [46]. The resulting network interconnects the polymer chains, thus increasing the cross-linking density and restricting the mobility of the polymer chains [17, 48, 49]. Accordingly, the T_g of the resulting composite material increases. Unlike the 0.5 wt% CNT system, the observed enhancement in the T_g due to better dispersion is more pronounced in composites with 0.25 wt% nanotube content. One may suggest that dispersion of higher CNTs in the resin matrix could alter the rate of polymerization, and thus, an effective enhancement of the T_g cannot be achieved, even at the optimum dispersion conditions.

Any adverse effect on the CNT dispersion quality is found to decrease the T_g of the nanocomposite. In a 0.25 wt% CNT system, the remarkable T_g drop at an energy level of 80 kJ can be attributed to the observed re-agglomeration process. It is well-established [18] that in resins polymerized via free radicals such as VE, the free radicals generated by decomposition of initiator (MEKP) can be easily entrapped within the galleries of entangled nanotubes. Therefore, one could presume that the more amount of free radicals may have probably entrapped within the galleries of larger CNT agglomerates. The latter can reduce the cross-linking density, particularly in the vicinity of the agglomerates [21], and dramatically decrease the T_g of the composite material.

The observed mechanical and thermal behavior of the nanocomposites at different sonication energies suggests that at both nanotube contents, the elastic modulus and T_g increase with sonication energy. However, there is a certain energy level, threshold energy, which results in the

maximum thermo-mechanical properties. Inducing sonication energies beyond this threshold level will cause deterioration of the material properties. The threshold energy level is ~ 60 kJ in case of 0.25 wt% CNT content, while it is ~ 15 kJ with 0.5 wt% CNT concentration. SEM micrographs clearly demonstrate that with higher CNT content, an extensive nanotube length reduction is inevitable, even at the early stage of sonication. This reduction in CNT aspect ratio is believed to limit the threshold energy to lower levels.

Conclusions

A thorough investigation has been performed to examine the role of sonication energy in the dispersion of carbon nanotubes into a vinyl ester resin. The study also determines as to how dispersion condition affects thermo-mechanical properties of nanocomposites. Mechanical properties such as elastic modulus and creep deformation have been estimated by three-point flexure and nanoindentation methods. Glass transition temperature has also been determined by differential scanning calorimetry. It has been observed that at a particular sonication energy level, CNT dispersion is optimum that provides the highest properties. This energy level has been termed as threshold energy meaning that sonication time and amplitude must correspond to this energy level to yield the most optimized dispersion and hence the maximum enhancement in properties. It has been observed that at this threshold energy level, the T_g and elastic modulus of the pure VE polymer can be enhanced by 13 °C and 24 %, respectively. It is also observed that sonication threshold energy is linked with the concentration of nanoparticles. The lower the concentration, the higher is the threshold energy level. SEM observations suggest that this threshold energy is controlled by

destruction of CNT structure. At higher nanotube contents, the threshold energy is reduced since a higher number of nanotubes are damaged even with a low energy input.

References

- Jancar J, Douglas JF, Starr FW, Kumar SK, Cassagnau P, Lesser AJ, Sternstein SS, Buehler MJ (2010) Current issues in research on structure–property relationships in polymer nanocomposites. *Polymer* 51:3321–3343
- Rahmat M, Hubert P (2011) Carbon nanotube–polymer interactions in nanocomposites: a review. *Compos Sci Technol* 72:72–84
- Thostenson ET, Ren Z, Chou TW (2001) Advances in the science and technology of carbon nanotubes and their composites: a review. *Compos Sci Technol* 61:1899–1912
- Coleman JN, Khan U, Blau WJ, Gun'ko YK (2006) Small but strong: a review of the mechanical properties of carbon nanotube–polymer composites. *Carbon* 44:1624–1652
- Desai AV, Haque MA (2005) Mechanics of the interface for carbon nanotube–polymer composites. *Thin-Walled Struct* 43:1787–1803
- Spitalsky Z, Tasis D, Papagelis K, Galiotis C (2010) Carbon nanotube–polymer composites: chemistry, processing, mechanical and electrical properties. *Prog Polym Sci* 35:357–401
- Ma PC, Siddiqui NA, Marom G, Kim JK (2010) Dispersion and functionalization of carbon nanotubes for polymer-based nanocomposites: a review. *Compos Part A* 41:1345–1367
- Byrne MT, Gun'ko YK (2010) Recent advances in research on carbon nanotube–polymer composites. *Adv Mater* 22:1672–1688
- Song K, Zhang Y, Meng J, Green EC, Tajaddod N, Li H, Minus ML (2013) Structural polymer-based carbon nanotube composite fibers: understanding the processing–structure–performance relationship. *Materials* 6:2543–2577
- Sabba Y, Thomas EL (2004) High-concentration dispersion of single-wall carbon nanotubes. *Macromolecules* 37:4815–4820
- Xie XL, Mai YW, Zhou XP (2005) Dispersion and alignment of carbon nanotubes in polymer matrix: a review. *Mater Sci Eng R* 49:89–112
- Grady BP (2010) Recent developments concerning the dispersion of carbon nanotubes in polymers. *Macromol Rapid Commun* 31:247–257
- Huang YY, Terentjev EM (2012) Dispersion of carbon nanotubes: mixing, sonication, stabilization, and composite properties. *Polymers* 4:275–295
- Hilding J, Grulke EA, Zhang ZG, Lockwood F (2003) Dispersion of carbon nanotubes in liquids. *J Dispers Sci Technol* 24:1–41
- Ahir SV, Huang YY, Terentjev EM (2008) Polymers with aligned carbon nanotubes: active composite materials. *Polymer* 49:3841–3854
- Thostenson ET, Ziaee S, Chou TW (2009) Processing and electrical properties of carbon nanotube/vinyl ester nanocomposites. *Compos Sci Technol* 69:801–804
- Seyhan AT, Gojny FH, Tanoğlu M, Schulte K (2007) Rheological and dynamic-mechanical behavior of carbon nanotube/vinyl ester–polyester suspensions and their nanocomposites. *Eur Polym J* 43:2836–2847
- Seyhan AT, Tanoğlu M, Schulte K (2009) Tensile mechanical behavior and fracture toughness of MWCNT and DWCNT modified vinyl-ester/polyester hybrid nanocomposites produced by 3-roll milling. *Mater Sci Eng A* 523:85–92
- Fan Z, Hsiao KT, Advani SG (2004) Experimental investigation of dispersion during flow of multi-walled carbon nanotube/polymer suspension in fibrous porous media. *Carbon* 42:871–876
- Fan Z, Advani SG (2005) Characterization of orientation state of carbon nanotubes in shear flow. *Polymer* 46:5232–5240
- Gryshchuk O, Karger-Kocsis J, Thomann R, Kónya Z, Kiricsi I (2006) Multiwall carbon nanotube modified vinyl ester and vinyl ester–based hybrid resins. *Compos Part A* 37:1252–1259
- Liao SH, Hung CH, Ma CCM, Yen CY, Lin YF, Weng CC (2008) Preparation and properties of carbon nanotube-reinforced vinyl ester/nanocomposite bipolar plates for polymer electrolyte membrane fuel cells. *J Power Sources* 176:175–182
- Liao SH, Hsiao MC, Yen CY, Ma CCM, Lee SJ, Su A, Tsai MC, Yen MY, Liu PL (2010) Novel functionalized carbon nanotubes as cross-links reinforced vinyl ester/nanocomposite bipolar plates for polymer electrolyte membrane fuel cells. *J Power Sources* 195:7808–7817
- Avilés F, Cauich-Rodríguez JV, Rodríguez-González JA, May-Pat A (2011) Oxidation and silanization of MWCNTs for MWCNT/vinyl ester composites. *Express Polym Lett* 5:766–776
- ASTM D790-10 (2010) Standard test methods for flexural properties of unreinforced and reinforced plastics and electrical insulating materials. ASTM International, West Conshohocken, PA. doi:10.1520/D0790-10
- ASTM E2546-07 (2007) Standard practice for instrumented indentation testing. ASTM International, West Conshohocken, PA. doi:10.1520/E2546-07
- Poveda R, Gupta N, Porfiri M (2010) Poisson's ratio of hollow particle filled composites. *Mater Lett* 64:2360–2362
- Oliver WC, Pharr GM (1992) An improved technique for determining hardness and elastic modulus using load and displacement sensing indentation experiments. *J Mater Res* 7:1564–1583
- ASTM E1356-08 (2014) Standard test method for assignment of the glass transition temperatures by differential scanning calorimetry. ASTM International, West Conshohocken, PA. doi:10.1520/E1356
- Mallick PK (2007) Fiber-reinforced composites: materials, manufacturing, and design, 3rd edn. CRC Press, Boca Raton
- Shtein M, Nativ R, Lachman N, Wagner HD, Regev O (2013) Fracture behavior of nanotube–polymer composites: insights on surface roughness and failure mechanism. *Compos Sci Technol* 87:157–163
- Kim MG, Moon JB, Kim CG (2012) Effect of CNT functionalization on crack resistance of a carbon/epoxy composite at a cryogenic temperature. *Compos Part A* 43:1620–1627
- Shokrieh MM, Hosseinkhani MR, Naimi-Jamal MR, Tourani H (2013) Nanoindentation and nanoscratch investigations on graphene-based nanocomposites. *Polym Test* 32:45–51
- Iijima M, Muguruma T, Brantley WA, Mizoguchi I (2011) Comparisons of nanoindentation, 3-point bending, and tension tests for orthodontic wires. *Am J Orthod Dentofac Orthop* 140:65–71
- Martinez R, Xu LR (2014) Comparison of the Young's moduli of polymers measured from nanoindentation and bending experiments. *MRS Commun* 4:89–93
- Gkikas G, Barkoula NM, Paipetis AS (2012) Effect of dispersion conditions on the thermo-mechanical and toughness properties of multi walled carbon nanotubes-reinforced epoxy. *Compos Part B* 43:2697–2705
- Montazeri A, Chitsazzadeh M (2014) Effect of sonication parameters on the mechanical properties of multi-walled carbon nanotube/epoxy composites. *Mater Des* 56:500–508
- Hull D, Clyne TW (1996) An introduction to composite materials, 2nd edn. Cambridge University Press, Cambridge

39. Ma PC, Kim JK, Tang BZ (2007) Effects of silane functionalization on the properties of carbon nanotube/epoxy nanocomposites. *Compos Sci Technol* 67:2965–2972
40. Siddiqui NA, Woo RSC, Kim JK, Leung CCK, Munir A (2007) Mode I interlaminar fracture behavior and mechanical properties of CFRPs with nanoclay-filled epoxy matrix. *Compos Part A* 38:449–460
41. Karapappas P, Vavouliotis A, Tsotra P, Kostopoulos V, Palpetis A (2009) Enhanced fracture properties of carbon reinforced composites by the addition of multi-wall carbon nanotubes. *J Compos Mater* 43:977–985
42. Li J, Ma PC, Chow WS, To CK, Tang BZ, Kim JK (2007) Correlations between percolation threshold, dispersion state, and aspect ratio of carbon nanotubes. *Adv Funct Mater* 17:3207–3215
43. Chakraborty AK, Plyhm T, Barbezat M, Necola A, Terrasi GP (2011) Carbon nanotube (CNT)–epoxy nanocomposites: a systematic investigation of CNT dispersion. *J Nanopart Res* 13:6493–6506
44. Mukhopadhyay K, Dwivedi CD, Mathur GN (2002) Conversion of carbon nanotubes to carbon nanofibers by sonication. *Carbon* 40:1373–1376
45. Battisti A, Skordos AA, Partridge IK (2009) Monitoring dispersion of carbon nanotubes in a thermosetting polyester resin. *Compos Sci Technol* 69:1516–1520
46. Tehrani M, Safdari M, Al-Haik MS (2011) Nanocharacterization of creep behavior of multiwall carbon nanotubes/epoxy nanocomposite. *Int J Plast* 27:887–901
47. Yang J, Zhang Z, Friedrich K, Schlarb AK (2007) Creep resistant polymer nanocomposites reinforced with multiwalled carbon nanotubes. *Macromol Rapid Commun* 28:955–961
48. Abdalla M, Dean D, Adibempe D, Nyairo E, Robinson P, Thompson G (2007) The effect of interfacial chemistry on molecular mobility and morphology of multiwalled carbon nanotubes epoxy nanocomposite. *Polymer* 48:5662–5670
49. Kathi J, Rhee KY, Lee JH (2009) Effect of chemical functionalization of multi-walled carbon nanotubes with 3-aminopropyltriethoxysilane on mechanical and morphological properties of epoxy nanocomposites. *Compos A* 40:800–809